

FROM REJECTION TO TRANSMISSION WITH STACKED ARRAYS OF SPLIT RING RESONATORS

J. Carbonell

Wave Phenomena Group, Departamento de Ingeniería Electrónica
Universidad Politécnica de Valencia, Camino de Vera, s/n
Valencia E-46022, Spain

E. Lheurette and D. Lippens

Institut d'Électronique de Microélectronique et Nanotechnologies
UMR CNRS 8520, Université des Sciences et Technologies de Lille
Avenue Poincaré BP 60069, Villeneuve d'Ascq Cedex 59652, France

Abstract—We report on free space transmission experiments carried out on stacked split ring resonator (SRRs) arrays operating at microwave frequencies. We start from the case of a single frequency selective surface which exhibits a rejection at the SRR resonance frequency. By stacking SRR arrays in the propagation direction, we then show experimentally the possibility to induce a transmission band just below this resonance frequency. Full wave analysis shows the role played by the longitudinal and transverse coupling effects in the electromagnetic properties of such bulk metamaterials, with the appearance of a transmission band resulting from an artificial magnetic activity.

1. INTRODUCTION

In the last few years, artificial magnetism has fueled a huge research effort in connection with the study of micro-structured artificial media, also termed metamaterials. These structures provide unique features such as those used in negative refraction devices [1], super-resolution lenses [2], or cloaking shells [3]. It has been very common to analyze them in terms of the EM properties of a unit cell, sometimes neglecting the interactions between the elementary constitutive elements. In addition, they are usually fabricated with planar arrays stacked in

a direction perpendicular to the wave propagation (with an in-plane wave vector \mathbf{k} and axial magnetic field H with respect to the resonant particles). Under this condition, they are operating under grazing incidence (in practice parallel to the stacked surfaces), which can be troublesome for practical use. In this paper, we address the problem of normal incidence on a stack of split ring resonators (SRRs) arrays by seeking a transparency condition (with full transmission) in a frequency range close to their resonant frequency. This effect is related to the possibility of generating an artificial magnetic response. The SRR acronym refers here to a single open ring resonator, as opposed to the more widely employed double ring structure. To this aim, we start from the experimental characterization under normal incidence of a one layer arrangement of SRRs, i.e., a frequency selective surface (FSS), which exhibits a typical rejection behavior (minimum transmission around the resonance frequency of the SRR). The signature of transverse coupling between the mesh elements can be clearly pointed out by varying the periodicity of the mesh. Basically, this lateral or transverse coupling can be related to the excitation and propagation of magneto-inductive (MI) waves on the SRR surface [4–7]. These MI waves can be compared to the surface plasmon waves in optics or ‘spoof plasmons’ at lower frequencies. Afterwards, we have analyzed the experimental results achieved by stacking two SRRs along the propagation direction. It is shown that the coupling effects in the propagation direction play a key role with a hybridization of eigenstates. The combination of both types of couplings in the transverse and along the propagation directions explains the appearance of resonant transmission bands, in addition to the rejection aforementioned for a single FSS. In a first part, we report on the experiments carried under free space conditions at frequencies around 10 GHz. These experimental results are then analyzed with the calculation of the eigenmodes for the periodic case. At last, field and current mappings permit one to understand the transition from a rejection behavior to a transmission window. This behavior is notably explained through the generation of a magnetic activity via the lift of degeneracy of coupled plasmon resonators where the anti-symmetric mode is equivalent to a current loop induced by the magnetic incident field.

2. EXPERIMENTAL RESULTS

For all the SRR surfaces, the dimensions of the unit cell structure are: SRR lateral external size $l = 3.5$ mm, strip width $w = 0.6$ mm, gap $g = 0.6$ mm, and cell period $p = 4$ mm. The prototype layers were fabricated by mechanical milling of 35 μm -thick copper foils coated on

one or two sides of a 0.508 mm-thick Neltec N9220 substrate (with approximate permittivity $\epsilon_r = 2.2$, and loss tangent $\tan \delta = 9.10^{-4}$ at 10 GHz). The pictures of a prototype and of the transmission experiment set-up are shown in Fig. 1. In practice, the samples are sandwiched between Rohacell foam plates ($\epsilon_r \approx 1$ at the operation frequencies) to press and hold together the stacked layers. For these free-space experiments, we employed broad band horns (4 to 40 GHz). The emitting and receiving antennas were respectively placed around 80 and 20 cm apart from the sample, in order to ensure as much as possible a plane wave incidence, while preserving a high dynamic at the output side.

Figure 2(a) shows the frequency dependence of S_{21} for a single SRR array measured between 4 and 14 GHz with a vector network analyzer. Measured data have been normalized with respect to the

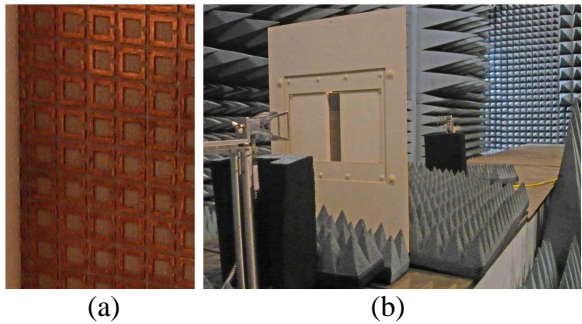


Figure 1. (a) Prototype SRR layer (zoomed view) and experimental setup (b) with a mounting support for the SRR layers.

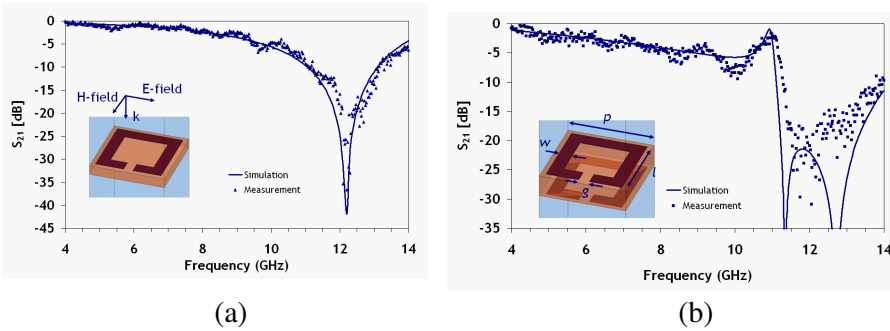


Figure 2. Measured and simulated transmission response of arrays of SRRs in single (a) and stacked (b) layers configurations. Insets show the unit cells with incident wave and characteristic dimensions.

measured free space path loss obtained without the presence of the sample. The main result is a dip (around -35 dB experimentally and -40 dB numerically) in the transmission curve at around 12.2 GHz, corresponding to an FSS-like response. Also plotted is the frequency dependence of the transmission coefficient calculated by full wave analysis. For these calculations we used the Maxwell equation solver HFSS from Ansoft. Master-slave boundary conditions have been employed for mimicking the transverse periodicity of the surface. A good agreement is achieved between numerical data and those calculated with a full wave analysis.

Figure 2(b) shows the variation of S_{21} as a function of frequency when two slabs, like the one previously characterized, are now stacked (actual substrate thickness is now $h = 1.016$ mm). First of all, it can be noticed in the simulation results that two zeros of transmission are now obtained around 11.3 and 12.7 GHz respectively. From the measurement point of view, it is not possible to distinguish them due to the limited dynamic range of the measurement setup, which is estimated around 65 dB (let us recall that measurements are normalized with respect to the free space path loss measured around 30 dB). The other salient result is the appearance of a narrow transmission window close to 11 GHz. Despite the fact the agreement between experimental and calculated data are not as good as in the aforementioned single layer case, the main features of the frequency dependence of the transmission are reproduced by the full wave analysis. Beyond the expected tolerance effect in experiment, it was also found that misalignment during the manual assembling stage could explain this disagreement.

3. NUMERICAL RESULTS AND DISCUSSION

Let us now consider the interpretation of the electromagnetic properties for the single and the double stacked layers respectively. In the case of a single SRR surface layer, a plane wave incident on the surface will typically exhibit a frequency selective behavior with a deep rejection at the vicinity of the resonance frequency of the resonator. A TE polarization is applied to the incident wave with the E -field orientation parallel to the ring gap. At resonance, there are strong surface currents on the metallic motif, with a half-wavelength matching the perimeter of the C-shaped strip. It is worth mentioning that these surface currents result from the *electromotive force* across the gap and not from the incident magnetic field, which has here an improper polarization direction, being parallel to the SRR plane (see insets of Fig. 2). In other words, there is no artificial magnetism and

the dip which is evidenced in the transmission spectrum results from an electrical activity. In terms of material parameters, and even if that may be however questionable for a metasurface, it would correspond to a ‘negative permittivity’ effect. This is also the basis for considering this surface being of a capacitive type, opposed to or dual of the inductive type, with the main difference of being transparent at low frequencies (capacitive) instead of opaque (inductive) [8].

In the case of the double stacked layer, the elementary resonators are not solely coupled in the transverse direction (MI transverse waves) but also along the direction of propagation. Under the condition of tight coupling between the resonators, via a thin spacer layer, there is a lift of degeneracy of eigenmodes. In the plasmonics community, this *lift of degeneracy* of the eigenstates is described as a *hybridization* effect with symmetric and antisymmetry modes [9, 10]. The lowest energy state corresponds to the anti-symmetric mode simulated here at 11 GHz as illustrated in Fig. 3(a). The reversal of the current direction in facing arms is equivalent to a current loop in the propagation direction induced by the incident H -field and not by the E -field as in the case of an FSS-like structure.

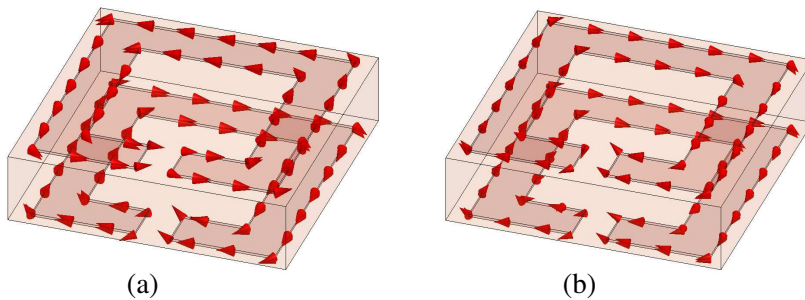


Figure 3. Surface current distributions from numerical simulations for a stacked layers structure (a) 11 GHz, anti-symmetric, and (b) 12.4 GHz, symmetric.

In order to confirm such a magnetic activity, Fig. 4 displays a unit cell of the stacked configuration with the mapping of the H -field on the central propagation plane (stacking direction). The directions of current streams are reported from numerical simulations in Fig. 4(a). They flow in opposite directions in both rings and the H -field lines have an *orientation change* across the dielectric spacer. For the higher anti-resonant frequency (dip in the transmission) around 12.4 GHz, the current flows in the same direction correspond to an electrical activity, as shown in Fig. 3(b).

At this stage it can be concluded that the stack of two layers

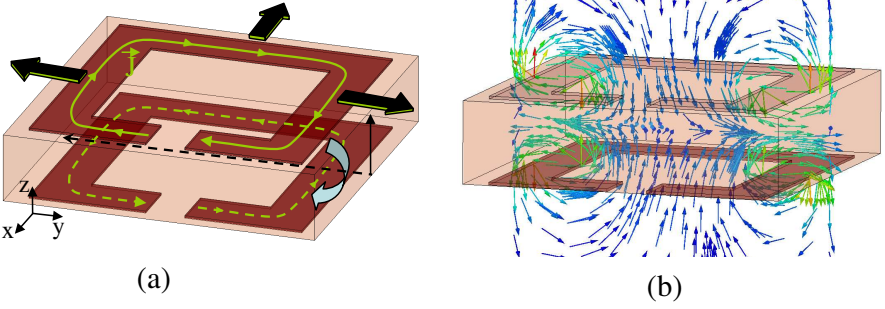


Figure 4. (a) Schematic unit cell of the stacked SRR structure with 2 layers. Arrows show transverse (at the surface level) and longitudinal (inter-surface) couplings. Surface current directions are displayed with anti-parallel directions on both rings. A central cut plane is also marked where in (b) H -field mapping is displayed at the resonance frequency of the 2 SRR layer stack (at 10.6 GHz).

permits one to create a resonant magnetic and electric dipoles with negative values of μ_{eff} and ε_{eff} . However, this happens at two *distinct* frequencies while a double negative media requires an overlap between them. As partial conclusion, the demonstration of electrical and magnetic activities is not sufficient to conclude to the achievement of a negative index material. Over the past, this difficulty was overcome notably with the addition of metal strips [11] or by an asymmetric alignment of paired cut wires. In the present case, the combined coupling in the transverse and the propagation direction, illustrated by the straight and curved arrows respectively, is responsible of a transmission window with the propagation of backward wave (negative index material). Such a finding, which results from the propagation of surface plasmon wave and anti-symmetrical coupling, was already demonstrated in stacked holes arrays operating at Terahertz frequencies with a clear experimental evidence of a phase advance [12,13]. The present structure can be considered as a dual structure of a stacked holes array according to the Babinet principle [14,15], with the added benefit of transverse compactness due to the use of SRRs arrays.

Let us also mention that this situation is also complementary to the one reported in [16], where the combination of dual FSSs (of inductive type such as perforated metallic plates and of capacitive type with resonant metallic elements, as the ones analyzed here) could also exhibit tunneling effects. Fig. 5, shows the calculated dispersion diagram of this stacked configuration by using the eigenmode solver

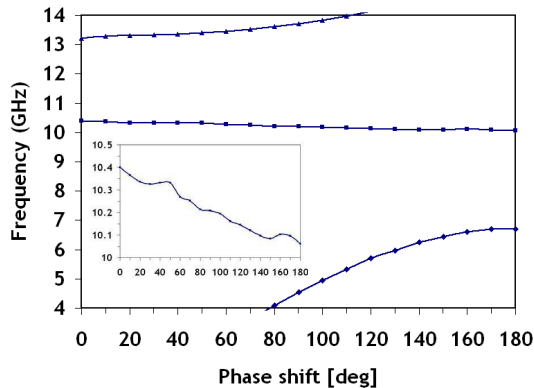


Figure 5. Calculated dispersion diagram for a two stacked SRR layers configuration. Inset shows zoomed view of the narrow bandwidth backward mode.

of HFSS. A very narrow bandwidth transmission mode is generated below the resonance frequency of the isolated SRR, slightly above 10 GHz, corresponding to the transmission peak reported in Fig. 2(b). Additionally to the conclusions from the illustrated field mappings, this propagation mode shows a negative slope in the dispersion diagram around the operating frequency (zoomed in inset), which confirms the backward wave propagation. This resonant mode is associated to a MI wave effect created in each SRR surface, by proximity coupling [17]. In other words, the surface MI waves in the up layer interface are coupled to the bottom one by mixing inductive and capacitive contributions. The field plot in Fig. 4 is a proof of this surface wave ‘translation’ from the first to the second interface of the device. As a last comment it is worth mentioning that the reversal of the magnetic field orientation pointed out by the field mapping in Fig. 4 is different from those found in *axially stacked resonators* which produce forward MI waves [17].

Finally, Fig. 6 shows two E -field plots corresponding to a 3 layer stack structure of finite size in the lateral dimension (here it is 15 cells wide). An incident quasi-plane wave from the top side impinges onto the top face of the microstructure. The simulation domain is laterally bounded by absorbing boundary layers (of PML type). Graphically, it is demonstrated that the stacked surfaces can be opaque or transparent to the incident wave depending on the excitation frequency. Under reflection conditions the wave does not penetrate beyond the first interface, whereas under transmission conditions, a uniform E -field distribution is generated in the full width of the device, with maximum

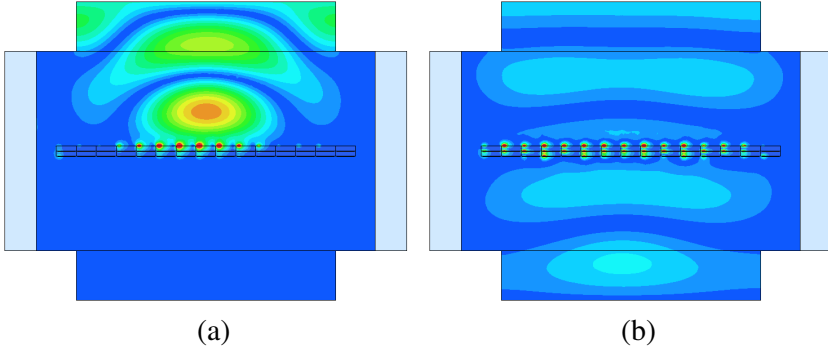


Figure 6. *E*-field patterns for a 15-cell wide, 3 layers stack prototype, top view, (a) rejection condition at 12.5 GHz, (b) transmission condition at 10.5 GHz.

E-field values corresponding to the slit locations. It is interesting to note that only the central part of the device has high field concentration in the opaque case, and also that only the first layer (the top one) is mainly contributing to the reflection of the impinging wave. This is a characteristic related to the resonant particle itself, and not to an interaction between the elements in the mesh. On the contrary, for the transparency frequency, all layers have significant intensities of electric field, both on the longitudinal and transverse directions. It is therefore a composite and collective behavior. This field pattern behavior demonstrates the coherency of the previous discussions especially of the bidirectional couplings established in the multilayer structures.

4. CONCLUSION

Experimental results combined with full wave simulations prove that the typical rejection behavior associated to capacitive-type frequency selective surfaces can be reversed to obtain transmission bands slightly below the resonance frequency of the elements on the surface. The control of the coupling along the transverse and propagation direction for a stacked SRR surface slab allows defining transmission bands for normal incident waves with backward resonant modes. Extension of these concepts to terahertz frequencies is currently being considered taking into account the drawback of dispersion in the metals response [18], with the target of developing imaging devices.

ACKNOWLEDGMENT

The authors acknowledge the assistance of Mr. Antonio Vila in the fabrication of the prototypes. J. C. acknowledges the financial support of MICINN, Spain (Contract numbers: TEC 2007-67239 and Consolider CSD2008-00066) and also USTL (France).

REFERENCES

1. Shelby, R. A., D. R. Smith, and S. Schultz, "Experimental verification of a negative index of refraction," *Science*, Vol. 292, 77–79, Apr. 2001.
2. Pendry, J. B., "Negative refraction makes a perfect lens," *Physical Review Letters*, Vol. 85, 3966–3969, Oct. 2000.
3. Schurig, D., J. J. Mock, B. J. Justice, S. A. Cummer, J. B. Pendry, A. F. Starr, and D. R. Smith, "Metamaterial electromagnetic cloak at microwave frequencies," *Science*, Vol. 314, 977–980, Oct. 2006.
4. Kozyrev, A. B., C. Qin, I. V. Shadrivov, Y. S. Kivshar, I. L. Chuang, and D. W. van der Weide, "Wave scattering and splitting by magnetic metamaterials," *Optics Express*, Vol. 15, 11714–11722, Aug. 2007.
5. Shamonina, E., V. A. Kalinin, K. H. Ringhofer, and L. Solymar, "Magnetoinductive waves in one, two, and three dimensions," *Journal of Applied Physics*, Vol. 92, 6252–6261, Nov. 2002.
6. Solymar, L. and E. Shamonina, *Waves in Metamaterials*, Oxford University Press, Oxford, 2009.
7. Carbonell, J., V. E. Boria, and D. Lippens, "Nonlinear effects in split ring resonators loaded with heterostructure barrier varactors," *Microwave Optical Technology Letters*, Vol. 50, 474–479, Feb. 2008.
8. Aznabet, M., M. Navarro-Cía, S. A. Kuznetsov, A. V. Gelfand, N. I. Fedorinina, Y. G. Goncharov, M. Beruete, O. El Mrabet, and M. Sorolla, "Polypropylene-substrate-based SRR- and CSRR metasurfaces for submillimeter waves," *Optics Express*, Vol. 16, No. 22, 18312–18319, Oct. 2008.
9. Prodan, E., C. Radloff, N. J. Halas, and P. Nordlander, "A hybridization model for the plasmon response of complex nanostructures," *Science*, Vol. 302, 419–422, Oct. 2003.
10. Kanté, B., S. N. Burokur, A. Sellier, A. de Lustrac, and J.-M. Lourtioz, "Controlling plasmon hybridization for negative

- refraction metamaterials,” *Physical Review B*, Vol. 79, 075121, Feb. 2009.
11. Guven, K., M. D. Caliskan, and E. Ozbay, “Experimental observation of left-handed transmission in a bilayer metamaterial under normal-to-plane propagation,” *Optics Express*, Vol. 14, No. 14, 8685–8693, Sep. 2006.
 12. Wang, S., F. Garet, K. Blary, C. Croënne, E. Lheurette, J. L. Coutaz, and D. Lippens, “Composite left/right-handed stacked hole arrays at submillimeter wavelengths,” *Journal of Applied Physics*, Vol. 107, 074510, 2010.
 13. Croenne, C., F. Garet, E. Lheurette, J. L. Coutaz, and D. Lippens, “Left handed dispersion of a stack of subwavelength hole metal arrays at terahertz frequencies,” *Applied Physics Letters*, Vol. 94, 133112, Apr. 2009.
 14. Beruete, M., M. Sorolla, and I. Campillo, “Left-handed extraordinary optical transmission through a photonic crystal of subwavelength hole arrays,” *Optics Express*, Vol. 14, 5445–5455, Jun. 2006.
 15. Ortuño, R., C. García-Meca, F. J. Rodriguez-Fortuño, J. Martí, and A. Martínez, “Role of surface plasmon polaritons on optical transmission through double layer metallic hole arrays,” *Physical Review B*, Vol. 79, 075425, Feb. 2009.
 16. Alú, A. and N. Engheta, “Evanescent growth and tunneling through stacks of frequency-selective surfaces,” *IEEE Antennas and Wireless Propagation Letters*, Vol. 4, 417–420, 2005.
 17. Shamonina, E., “Slow waves in magnetic metamaterials: History, fundamentals and applications,” *Physica Status Solidi*, Vol. 245, No. 8, 1471–1482, Jun. 2008.
 18. Liu, N., H. Guo, L. Fu, S. Kaiser, H. Schweizer, and H. Giessen, “Three-dimensional photonic metamaterials at optical frequencies,” *Nature Materials*, Vol. 7, 31–37, Jan. 2008.